Biosensors and Bioelectronics 124–125 (2019) 89–95

Contents lists available at ScienceDirect

Biosensors and Bioelectronics

journal homepage: www.elsevier.com/locate/bios

An electroanalysis strategy for glutathione in cells based on the displacement reaction route using melamine-copper nanocomposites synthesized by the controlled supermolecular self-assembly

Yue Hua, Min Liu, Shuai Li, Fengjuan Liu, Yuanyuan Cai, Huan Liu, Yuqi Wan, Xiaoxia Lv, Hua Wang*

Institute of Medicine and Materials Applied Technologies, College of Chemistry and Chemical, Engineering, Qufu Normal University, Qufu City, Shandong Province 273165, PR China

ARTICLE INFO

Keywords:
Supermolecular self-assembly
Melamine-copper nanorods
Solid-state CuCl electrochemistry
Electroanalysis
Glutathione

ABSTRACT

An electroanalysis strategy has been developed for probing glutathione (GSH) separately in hela and yeast cells based on the displacement reaction route using melamine-copper (MA-Cu) nanocomposites. Herein, MA-Cu nanocomposites were initially synthesized by the controlled supermolecular self-assembly process showing various morphological structures depending on the MA-to-Cu ratios used. It was discovered that the electrodes modified with rod-like MA-Cu nanocomposites could achieve the stable electrochemical output of solid-state CuCl at a low potential, which might circumvent the possible interference from co-existing electroactive substances in complicated backgrounds like cells. More importantly, the yielded CuCl signals would decrease selectively induced by GSH through the specific Cu-GSH interaction that would trigger the displacement of CuCl into non-electroactive complex. The MA-Cu nanorods-modified electrodes can allow for the detection of GSH with the concentrations linearly ranging from 0.010 to 300.0 μM. Subsequently, the feasibility of the developed electroanalysis strategy was demonstrated for the evaluation of GSH separately in the extractions of hela and yeast cells, promising the wide applications in the clinical and food analysis fields.

1. Introduction

Glutathione (GSH), which is a tripeptide composing of glutamicacid, cysteine, and glycine, (Lv et al., 2016) plays the critical roles in many physiological processes such as reversible redox reactions (Ju et al., 2014; Niu et al., 2012; Xu and Hepel, 2011; Yuan et al., 2013; Zhang et al., 2016; Zhu et al., 2013). Abnormal levels of intracellular GSH can be highly relative to some serious diseases such as cancers, diabetes, Parkinson's disease, and carcinogenesis (Niu et al., 2012; Xu and Hepel, 2011; Zhang et al., 2016; Zhu et al., 2013). Especially, GSH may induce the apoptosis of cancer cells in the early stage (Zhang et al., 2016). Also, GSH has been used as the potential antidote for removing heavy metal ions like copper ions because of their strong interactions (Cruz et al., 2001; Sun et al., 2016). In addition, GSH in yeast cells can endow them the abilities of detoxification and anti-oxidization, so that they are widely applied in the food industry. Therefore, developing some sensitive and selective analysis methods to monitor GSH levels under different cellular physiological conditions are of significant interest in the clinical and food analysis fields (Tsardaka et al., 2013; Yin et al., 2014).

Over the past decades, a variety of analytical techniques have been applied for probing GSH in different biological media, typically as high-performance liquid chromatography, mass spectrometry, colorimetry, and fluorescent techniques (Detsri and Seeharaj, 2017; Gu et al., 2015; Kanďár et al., 2013). Moreover, most of these reports have focused on the detections of GSH in blood (Hakuna et al., 2015; Squellerio et al., 2012), whereas the evaluation of intracellular GSH has been generally conducted by cell imaging (Gutscher et al., 2008; Kong et al., 2016; Sousa et al., 2012). Yet, they may involve the complicated operation, bulky instrumentation, and cumbersome laboratory procedures, which may largely limit their clinical applications (Hu et al., 2013). Therefore, developing a simple, sensitive, selective, and field-deployable detection method for probing GSH especially those in cells has become an attractive and challenging target. Electrochemical detection technologies, with high detection sensitivity, easy operation, and portable devices suitable for the on-site applications (Li et al., 2015; Si et al., 2014), have been alternatively applied for the detection of GSH in blood (Kanďár et al., 2013; Miao et al., 2009; Safavi et al., 2009; Shahmiri et al.,

* Corresponding author.
E-mail address: huawang@qfnu.edu.cn (H. Wang).

https://doi.org/10.1016/j.bios.2018.10.022
Received 21 August 2018; Received in revised form 27 September 2018; Accepted 11 October 2018
Available online 13 October 2018
0956-5663/

2013). Miao et al. described an electrochemical strategy for sensing GSH using complementary thiolated oligonucleotides (Miao et al., 2009). Shahmiri and co-workers designed an ethynylferrocene nanocomposite modified electrode as a novel voltammetric sensor for simultaneous determination of GSH and acetaminophen (Shahmiri et al., 2013). Safavi *et al.* have reported an electrochemical determination of GSH at a copper hydroxide nanocomposite electrode (Safavi et al., 2009). Nevertheless, these current electroanalysis methods may suffer from the complicated modification process of electrodes, and especially the analysis sensitivity might be largely restrained by the direct electrochemical responses to analytes on the electrode surfaces (Lv et al., 2016).

Recent years have witnessed the wide applications of copper (Cu) nanomaterials for the design of various electrochemical sensors by taking some advantages of high electron transferring and electrochemical redox activities towards the desirable electroanalysis performances (Bretthollе et al., 2010; Shi et al., 2015). However, a challenge may be commonly encountered regarding the notorious inherent instability of Cu nanomaterials in water, which may prevent them from the applications on a large scale. Moreover, melamine (MA), an organic molecule consisting of three amino groups and three aromatic nitrogen atoms, can be readily polymerized as powerful adsorbents for the removal of some heavy metal ions (Tsoufis et al., 2012; Zhao et al., 2015). For example, Tan and co-workers reported a MA-formaldehyde polymer to remove some toxic metal ions from water (Tan et al., 2013). Our group also synthesized MA-silver nanomaterials for sensing sulfides in blood (Liu et al., 2017). Particularly, MA was established to display the considerably strong interaction with Cu^{2+} ions to act as the functional templates for preparing various Cu nanocomposites (Ghani et al., 2015; Tan et al., 2013).

In the present work, melamine-copper (MA-Cu) nanocomposites were synthesized initially by the controlled supermolecular self-assembly process, in which MA might serve as the reductant and protector. The resulted MA-Cu nanocomposites were demonstrated to present high aqueous stability, large surface area, and various morphological structures such as nanorods, nanowires and particles, depending on the MA-to-Cu ratios used. It was discovered that the electrodes modified with MA-Cu nanorods could display more stable electrochemical oxidation peaks of CuCl at a lower potential. Importantly, highly sensitive responses to GSH could be thus achieved through the specific Cu-GSH binding to trigger irreversible displacement reactions towards the conversion of CuCl into non-electroactive Cu-GSH complex, thus leading to the decrease in CuCl signals. Such a displacement reaction route can circumvent the limitations of sensing sensitivity for the most direct electrochemical responses to analytes. Subsequently, the practical electroanalysis of GSH in samples of hela and yeast cells was conducted. To the best of our knowledge, this is the first report on the electroanalysis of GSH in the extractions of hela and yeast cells samples based on the displacement reaction route of solid-state CuCl electrochemistry using MA-Cu nanocomposites, which were synthesized by the controlled supermolecular self-assembly process.

2. Experimental section

2.1. Reagents

Melamine (MA) and copper nitrate were purchased from Sinopharm Chemical Reagent Co. (China). Phosphate buffer saline (PBS) solution and glutathione (GSH) were obtained from Aladdin Reagent Co., Ltd. (Shanghai, China). Nafion solution (5.0%), dry yeast, alanine (Ala), glycine (Gly), phenylalanine (Phe), cysteine (Cys), ascorbic acid (AA), dopamine (DA), uric acid (UA), glucose (Glu), bovine serum albumin (BSA), fetal bovine serum, RIPA lysis buffer, and GSH assay kits were purchased from Sigma-Aldrich (Beijing, China). HeLa cells were purchased from Shanghai SunBio Biomedical technology Co., Ltd. All other reagents are of analytical grade. Deionized water (> 18 Mohm) was obtained from an ultrapure water system (Pall, USA). All glass containers were cleaned in turn by aqua regia and ultrapure water.

2.2. Apparatus

Scanning electron microscopy (SEM, Hitachi E-1010, Japan), X-ray photoelectron spectrometer (XPS, Thermo ESCALAB 250XI) and UV-3600 spectrophotometer (Shimadzu, Japan) were utilized for the characterization of the prepared materials. The MA-to-Cu ratios-dependent morphological structures of MA-Cu nanocomposites were also observed using inverted fluorescence microscope (Olympus, IX73-DP80, Japan). Electrochemical measurements were conducted with an electrochemical workstation CHI 760D (CH Instrument, Shanghai, China) connected to a personal computer. A three-electrode system was applied consisting of a gold working electrode, which was polished first with alumina powder and then ultrasonically cleaned with water and alcohol, a Pt wire counter electrode, and an Ag/AgCl reference electrode.

2.3. Synthesis of MA-Cu nanocomposites

The MA-Cu nanocomposites were synthesized by the controlled supermolecular self-assembly procedure using MA and copper nitrate at different molar ratios (16/1, 8/1, 4/1, 2/1, 1/1, 1/2, and 1/4). Briefly, MA (16.0 mM) was prepared using an aliquot of 0.010 g MA dissolved in 5.0 mL water at 60 °C, and then cooled down to room temperature. Under stirring, 5.0 mL copper nitrate of different concentrations (1.0, 2.0, 4.0, 8.0, 16.0, 32.0, and 64.0 mM) was separately added into 5.0 mL MA (16.0 mM) to be aged for 1 h to yield blue MA-Cu nanocomposites to be stored in dark. The composition of the resulting nanocomposites was analyzed by using X-ray photoelectron spectroscopy (XPS). In addition, optical fluorescent microscopy was employed to characterize the morphologies of the resulting MA-Cu nanocomposites after being dried on a glass plate.

2.4. Electroanalysis of GSH using the MA-Cu modified electrodes

The optimization of electroanalysis conditions of the MA-Cu nanorods modified electrodes for sensing GSH were conducted using different amount of MA-Cu nanorods (0.75, 0.85, 0.99, 1.19, 1.49, 1.99, and 2.98 mg/mL), pH values (1.0, 3.0, 5.0, 6.0, 7.0, 8.0, 9.0, 11, and 13), ionic strengths (20, 40, 60, 80, 100, 160, and 200 mM NaCl), and storage time of MA-Cu nanorods modified electrodes (1.0, 2.0, 4.0, 6.0, 8.0, 10, and 12 months).

Under the optimized conditions, the electroanalysis for GSH with the electrodes modified with MA-Cu nanorods were performed. Typically, an aliquot of 2.5 μL MA-Cu suspensions (1.19 mg/mL) in Nafion, which amount was optimized to be 5.0%, was dropped onto the gold electrodes to be air-dry for future usage. The linear sweep voltammetries (LSVs) were performed at the potentials ranging from - 0.20 to 0.60 V at a scanning speed of 100 mV/s. Further, the control tests were conducted accordingly with the MA-Cu modified electrodes using some other common ions and compounds (300.0 μM), including Cl^-, F^-, Br^-, Na^+, K^+, Ca^{2+}, Mg^{2+}, NH_4^+, Fe^{3+}, Ala, Gly, Phe, Cys, AA, DA, UA, Glu, and BSA. Subsequently, an aliquot of GSH with different concentrations (0–300.0 μM) was separately introduced into the optimized PBS (pH 7.0, containing 60.0 mM NaCl) for the electrochemical LSV measurements. Besides, according to the same procedure, the developed electroanalysis method was applied for the evaluation of intracellular GSH samples extracted separately from hela cells and yeast cells samples above, of which the extraction of intracellular GSH from hela and yeast cells was detailed in the Supplementary materials.

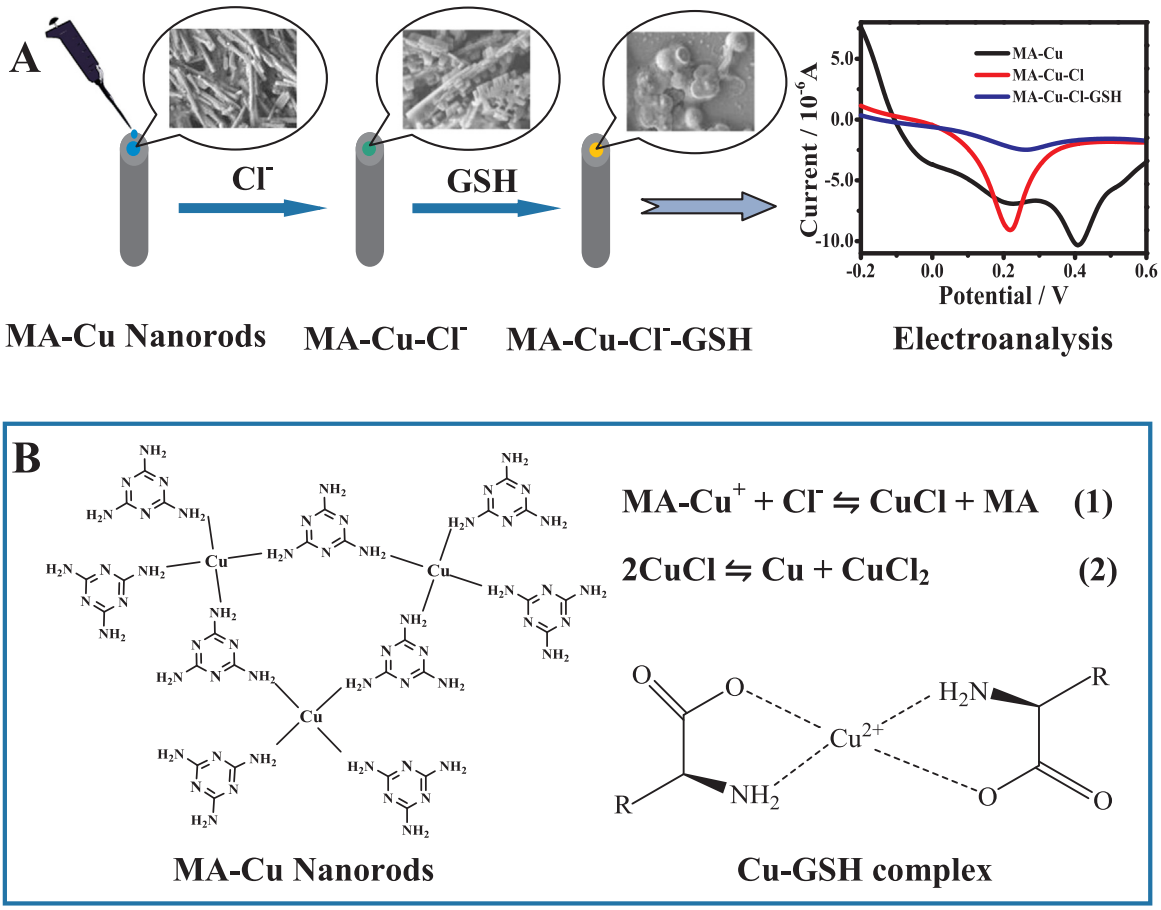

Scheme 1. Schematic illustration of (A) the step-by-step setup of the MA-Cu nanorods modified electrodes with the electrochemical responses to Cl^- ions and then GSH (top: SEM images of the resulting products); (B) the structural formula of MA-Cu nanorods prepared by the supermolecular self-assembly (left), in which the Cu-Cl reactions and Cu-GSH complex would undergo (right).

3. Results and discussion

3.1. Main sensing principle and procedure for the MA-Cu-based electroanalysis of GSH

The MA-Cu nanorods were prepared by the supermolecular self-assembly, in which MA might serve as the reductant and protector. They were further modified onto the electrodes for the GSH electroanalysis based on the solid-state CuCl electrochemistry. The main sensing principle and procedure are illustrated in Scheme 1. Scheme 1A discloses the step-by-step setup of the MA-Cu nanorods modified electrode with the electrochemical responses to Cl^- ions and then GSH, showing the changing CuCl signals. The morphological structures of the corresponding products would be varied, as revealed by their SEM images (top). Herein, Cu^+ in MA-Cu nanorods could interact with Cl^- ions to form CuCl, which would conduct the disproportionation reaction as manifested in Scheme 1B. When GSH was introduced, it would strongly chelate with Cu^{2+} ions to produce the Cu-GSH complex featuring the considerably stable tetragonal geometry (Sun et al., 2016). Accordingly, an electrochemical process might take place on the electrodes modified with MA-Cu nanorods regarding the Cu redox as follows:

$$MA\text{-}Cu^+ \text{ (solid)} + 2\ Cl^- \text{ (solution)} \leftrightharpoons CuCl_2 \text{ (solution)} + e^- \quad (1)$$

$$CuCl_2 \text{ (solution)} + e^- \leftrightharpoons CuCl \text{ (solid)} + Cl^- \text{ (solution)} \quad (2)$$

Herein, in a repetitive potential cycle, Cu^+ in MA-Cu was first oxidized to $CuCl_2$, which would be then reduced to CuCl in the reverse cathodic potential cycle. Furthermore, the addition of GSH would specifically trigger the GSH-chloride displacement reactions towards the conversion of CuCl into Cu-GSH complex with no electro-activity. As a result, a rational decrease in CuCl signals could be observed so as to facilitate the sensitive electroanalysis of GSH afterwards. In particular, the so proposed electroanalysis strategy by the displacement reaction route of solid-state electrochemistry would expect to overcome the limitations of detection sensitivity of the most direct electrochemical responses to analytes on the electrode surfaces.

3.2. Synthesis and characterization of MA-Cu nanocomposites

It was well established that MA with aromatic nitrogen atoms and amino groups could be polymerized showing the strong interaction with Cu^{2+} ions (Tsoufis et al., 2012; Ghani et al., 2015). Herein, the MA-Cu nanorods were synthesized by the controlled supermolecular self-assembly using Cu^{2+} ions and MA, with the structural formula illustrated in Scheme 1B. One can note from Fig. S1A that UV–vis spectra of the resulting MA-Cu nanorods can include the characteristic absorbance peaks of MA and Cu^{2+} ions (i.e., around 300 nm). Importantly, MA might serve as the reductant to facilitate the formation of Cu^+ ions in MA-Cu nanorods for the solid-state CuCl electrochemistry, which was evidenced by the CuCl precipitation reaction once adding Cl^- ions (Fig. S1B). Furthermore, the XPS analysis was carried out for the as-prepared MA-Cu nanorods with Cl^- ions to explore the composition and the chemical states of Cu atoms (Fig. S2). As shown in Fig. S2A, the $Cu2p_{3/2}$ and $Cu2p_{1/2}$ were obtained mainly peaking at 932.9 and 954.7 eV, respectively. As expected, the peak-fit of $Cu2p_{3/2}$ profile can be accompanied with a series of satellites of Cu^+ and Cu^{2+} elements, in which peak 1 refers to Cu^+ and peak 2, 3, and 4 belong to Cu^{2+} valent states

(Yin et al., 2010). Fig. S2B displays the total XPS of the MA-Cu nanorods with Cl^- ions including C 1s, N 1s, O 1s, Cl 2p, and Cu 2p, thus demonstrating the product consisting of five elements of C, N, O, Cl, and Cu. Moreover, the MA-Cu nanorods could have different morphological structures depending on the MA-to-Cu molar ratios, as revealed in the microscope images (Fig. S3). For instance, MA-Cu nanorods could be synthesized with increasing dendritic morphologies when increasing the MA-to-Cu molar ratios. Accordingly, the controlled supermolecular self-assembly route could enable the MA-Cu products to be formed with the varying morphological structures. Fig. S4A describes that the electrodes modified with MA-Cu nanorods could also exhibit the varying electrochemical CuCl signals depending on the MA-to-Cu ratios used in the fabrication, showing the highest CuCl signal at the MA-to-Cu ratio of 4/1 yielding the MA-Cu nanorods. More interestingly, one can note from that such a MA-to-Cu ratio could ensure the MA-Cu nanorods-modified electrodes with the largest response to the targeting GSH (Fig. S4B). Therefore the optimal MA-to-Cu ratio of 4/1 should be selected for forming the MA-Cu nanorods, of which the highest surface-to-volume ratios might be presumably expected for the high absorption of testing substances (i.e., Cl^- and GSH).

To explore the change of morphological structures, SEM imaging was conducted for the MA-Cu nanorods before and after the introduction of Cl^- ions and then GSH (Fig. 1). It was discovered that the so prepared MA-Cu nanocomposites could display the structural nanorods (Fig. 1A). Upon adding Cl^- ions, they could be broken to yield the dendritic blocks (Fig. 1B), which might be ascribed to the formation of CuCl precipitation through the interaction between Cl^- ions and Cu^+ in MA-Cu nanorods. When GSH were added further, to our surprise, spherical agglomerates were largely produced due to that the stronger Cu-GSH interactions that would trigger the displacement reaction between chloride and GSH could occur leading to the conversion of CuCl to Cu-GSH complex spheres (Fig. 1C).

3.3. Electrochemical sensing properties of the MA-Cu nanorods modified electrodes

The MA-Cu nanorods modified electrodes were employed for the electroanalysis for GSH through the solid-state CuCl electrochemistry. Fig. 2A shows the characteristic electrochemical linear sweep voltammetries (LSVs) of the MA-Cu nanorods modified electrodes before and after adding Cl^- ions, followed by addition of GSH, in comparison with the bare electrode and the MA-modified electrodes. It was found that after adding Cl^- ions, the MA-Cu nanorods modified electrode could present a larger CuCl oxidization peak at a low potential of about 0.22 V (curve b), in contrast to the one before adding Cl^- ions showing a Cu oxidization peak at about 0.41 V (curve a). Notably, this lower peak potential of CuCl oxidization would help to circumvent the possible interference from other electroactive backgrounds with the overlapped voltammetric signatures. In addition, the MA-modified electrode would exhibit no significant LSV signal. More importantly, the addition of GSH could induce the larger decrease in the CuCl current signals of the MA-Cu nanorods modified electrode (curve c). Fig. 2B illustrates the comparison of conductivity among the MA-Cu nanorods modified electrode, the MA-modified electrode, and the bare electrode in the $K_3[Fe(SCN)_6]$ probing solution. Unexpectedly, the cyclic voltammetric (CV) signals of the MA-Cu nanorods modified electrode can substantially approach to that of the bare electrode, which is much larger than that of the MA-modified electrode, indicating the considerably strong conductivity of MA-Cu nanorods. Furthermore, the addition of GSH could cause a decrease in the conductivity of the MA-Cu nanorods modified electrode. Moreover, Fig. S5A depicts that the peak currents of the developed electrode could increase linearly with the scan rates ranging from 50 to 400 mV/s. The results demonstrate that the CuCl oxidation reaction on the MA-Cu nanorods modified electrode should be a surface-controlled electrochemical process. In addition, the electrochemical sensing stability of the MA-Cu nanorods modified electrode was tested via continuous CV scanning for 100 cycles (Fig. S5B). Interestingly, the developed electrode could remain essentially the unchanged CV responses, demonstrating a desirably high electrochemical stability.

3.4. Optimization of GSH electroanalysis conditions

The effects of the MA-Cu dosages, pH values, NaCl amounts, and storage time on the electroanalysis performances of the MA-Cu nanorods modified electrodes for sensing GSH were investigated (Fig. S6). The results indicate that the GSH-induced current changes can increase with increasing MA-Cu dosages till 1.19 mg/mL, over which the current signals would gradually decrease (Fig. S6A). The phenomenon may presumably be attributed to the fact that much denser MA-Cu nanorods modifiers might be stacked onto the electrode surfaces, thus leading to the decrease in the conductivity. Accordingly, 1.19 mg/mL of MA-Cu nanorods was thought to be the optimal one in the experiments. Fig. S6B shows that the pH values could influence the CuCl signals. Obviously, higher CuCl peak currents at a lower potential could be obtained at pH 7.0, which should be selected as the most suitable one. Meanwhile, the CuCl peak currents could increase as NaCl concentrations increasing up to 60.0 mM, over which the current signals could gradually decrease, as clearly disclosed in Fig. S6C. Accordingly, 60.0 mM NaCl was chosen as the optimal for sensing GSH. Fig. S6D exhibits that the response time of the MA-Cu nanorods modified electrodes, revealing that the GSH response could be completed within 50 s.

3.5. Performances of GSH electroanalysis

The electroanalysis selectivity of the MA-Cu nanorods modified electrodes was explored for GSH, in comparison to the common ions and small molecules or amino acids possibly co-existing in hela and yeast cells (Fig. 3). One can note that all of the tested analytes alone could present the negligibly low responses, except for cysteine (Cys) (Fig. 3A). Interestingly, the compounds like S^{2-} ions, ascorbic acid (AA),

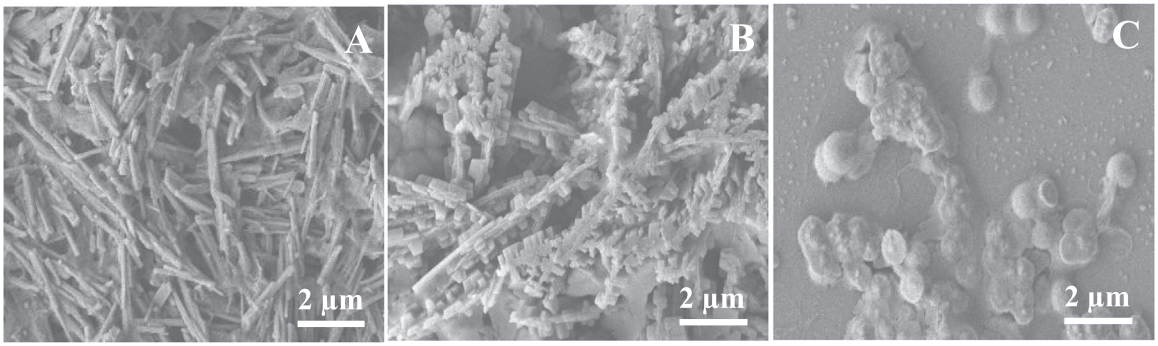

Fig. 1. The characteristic SEM images of MA-Cu nanorods in the (A) absence and the presence of (B) Cl^- ions, and (C) then GSH.

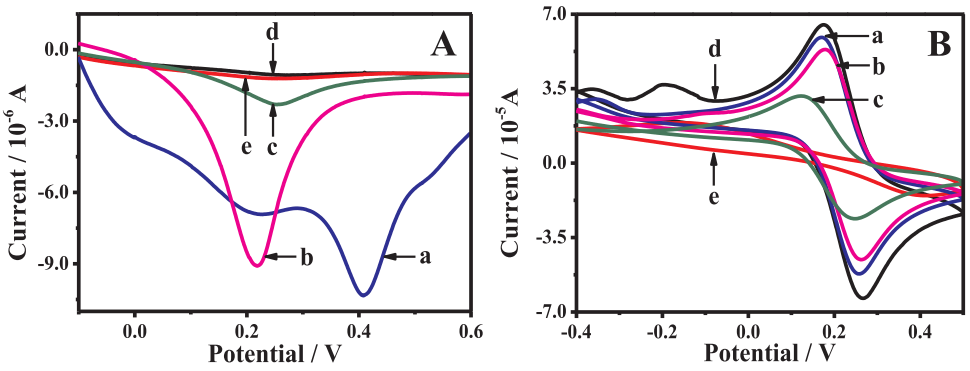

Fig. 2. (A) Characteristic electrochemical LSVs and (**B**) conductivity investigations with $K_3[Fe(SCN)_6]$ probes for the MA-Cu nanorods modified electrodes (a) before and (b) after adding Cl^- ions, and then (c) GSH, taking (d) the bare electrode and (e) the MA-modified electrodes as the controls.

and dopamine (DA) could increase. Moreover, Cys might display a noticeable response, which however is much lower than that of GSH at the same concentration. Furthermore, when these tested substances were separately mixed with GSH, they showed no significant effects on the GSH responses (Fig. 3B). Herein, the strong Cu-GSH interactions would induce the specific Cu-Cl displacement reactions to trigger the conversion of CuCl into Cu-GSH complex, thereby leading to a rational decrease in the CuCl signals. In one word, with the strong ability against interferences the developed electroanalysis method could selectively probe GSH in some complicated samples like hela and yeast cells extractions.

The detection reproducibility of the MA-Cu modified electrodes was evaluated in sensing GSH, showing the statistic standard deviation of 3.8% for the results obtained from the six MA-Cu-modified electrodes tested (Fig. S7A). Moreover, replicated detections were performed for the same sample, demonstrating the high sensing consistency of GSH responses (Fig. S7B). Besides, electrochemical investigations were carried out on the storage stability of MA-Cu nanorods (Fig. S7C). As expected, no significant change of CuCl signals was monitored for the electrodes modified with MA-Cu nanorods that were stored even up to 12 months. The data indicate that the developed electrochemical GSH sensor could present pretty high detection selectivity and reproducibility, in addition to the long-term stability of sensing nanocomposites.

3.6. Electroanalysis of GSH in samples

Under the optimized detection conditions, the developed electroanalysis method with MA-Cu nanorods was first applied for sensing GSH with different concentrations in buffer (Fig. 4). It was found that the current responses of the developed electrodes would decrease with the increasing GSH concentrations (Fig. 4A). A linear relationship was thus obtained for the electrochemical responses versus Log [GSH] concentrations ranging from 0.010 to 300.0 μM (Fig. 4B), with the limit of detection (LOD) of about 2.5 nM, estimated by 3σ rule. The sensing performances of the developed electroanalysis strategy were investigated by comparing with those of other kinds of GSH electroanalysis methods reported previously. The analysis results are comparably summarized in Table S1. One can note that the developed MA-Cu nanorods modified electrode can present the better detection performances in terms of the detection ranges and LODs. Therefore, the as-developed electroanalysis strategy may promise the practical applications for the ultrasensitive bioanalysis of GSH in various samples.

Moreover, the developed electroanalysis method with MA-Cu nanorods was practically employed to probe GSH separately in the extractions of hela and yeast cells samples. The linear relationships were obtained for the electrochemical responses versus Log [GSH] concentrations for the hela cells and yeast cells samples ranging from 0.025 to 280.0 μM (Fig. 4C) and 0.050–280.0 μM (Fig. 4D), respectively. Further, the recovery tests were also conducted by using the developed electroanalysis method to probe GSH separately in hela cells and yeast cells samples, showing the recoveries obtained ranging from about 97.5–106.5% (Table S2). The above results indicate that the application feasibility of the developed electroanalysis platform with MA-Cu nanorods can allow for the sensitive detections of GSH in the complicated samples like cells extractions.

4. Conclusions

In a summary, a highly sensitive and selective electroanalysis method has been successfully developed for sensing GSH separately in

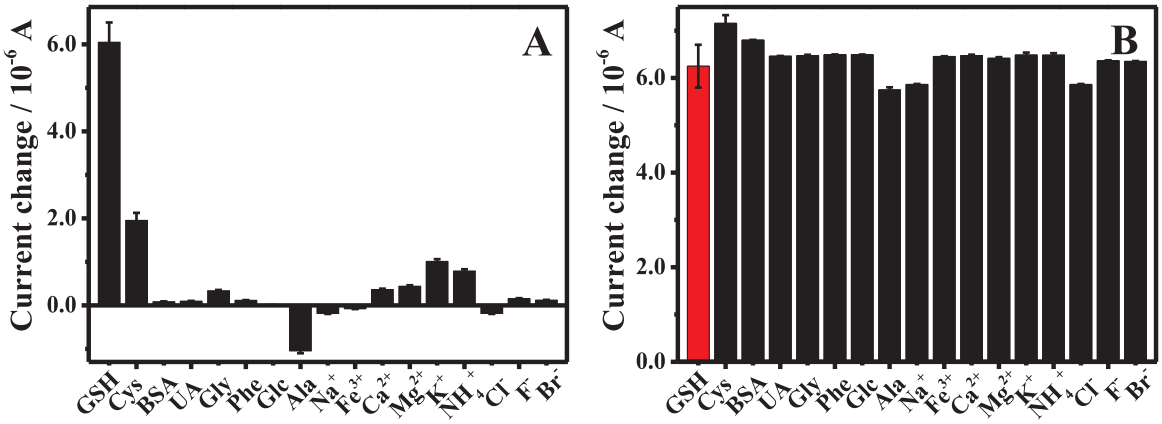

Fig. 3. Electrochemical LSV responses of the MA-Cu nanorods modified electrodes to (A) different interferents indicated alone, and (B) interferents mixed separately with GSH of same concentration (300.0 μM).

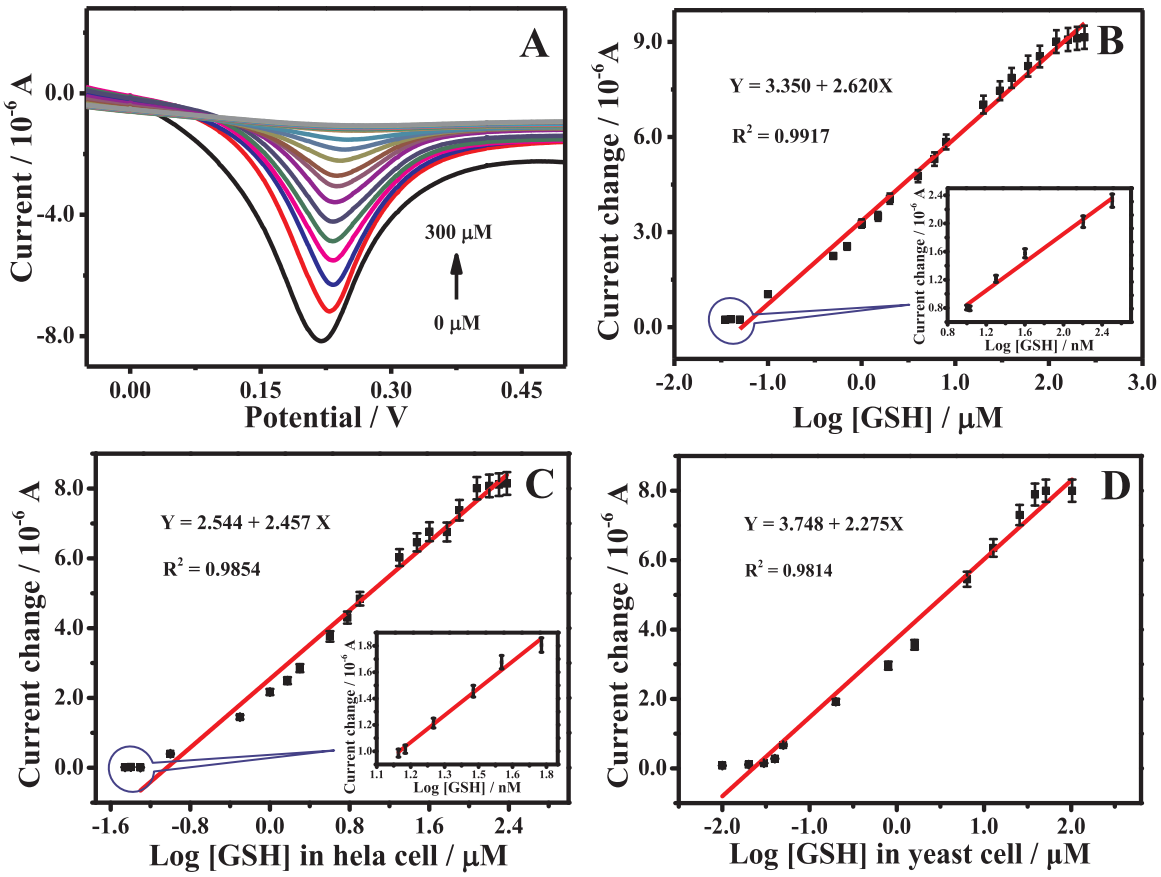

Fig. 4. (A) Electrochemical LSV responses to GSH of different concentrations in buffer measured at a sweep rate of 100 mV/s. (B) The calibration curve for the relationship between the current responses and different GSH concentrations. The calibration curve for the relationship between the current responses and different GSH concentrations in the extractions of (C) hela cells and (D) yeast cells samples.

the extractions of hela and yeast cells based on the displacement reaction route of solid-state CuCl electrochemistry. Herein, MA-Cu nanocomposites were synthesized for the first time by the controlled supermolecular self-assembly process showing various morphological structures. It was discovered that the electrodes modified with rod-like MA-Cu nanocomposites could obtain the stable output of solid-state CuCl electrochemistry at a desirably low potential, which may avoid the possible interference from electroactive substances co-existing in the complicated media like cells extractions. Moreover, highly sensitive detection of GSH could be realized through the specific Cu-GSH binding to trigger the displacement of CuCl into non-electroactive complex. More importantly, the as-developed electroanalysis strategy based on the displacement reaction route of solid-state CuCl electrochemistry may circumvent the limitations of detection sensitivity of the common direct responses to analytes on the electrode surfaces. This electroanalysis device equipped with the portable transducer can be tailored for the field-deployable monitoring of GSH under different cellular physiological conditions in the clinical, food, and environmental analysis fields. It should be pointed out that the developed electroanalysis method may be limited currently for the in-vitro detections of GSH in cells extractions or body fluids (i.e., blood and urine). In the future, the application of the electroanalysis sensor for the in-vivo analysis of GSH (i.e., the ones in single live cell) has been scheduled by using the miniaturized electrodes.

Acknowledgment

This work is supported by the National Natural Science Foundation of China (Nos. 21675099, 21375075, and 21601106), and Major Basic Research Program of Natural Science Foundation of Shandong Province, P R China (ZR2018ZC0129).

Appendix A. Supporting information

Supplementary data associated with this article can be found in the online version at doi:10.1016/j.bios.2018.10.022.

References

Brettholle, M., Höfft, O., Klarhöfer, L., Mathes, S., Mausfriedrichs, W., Zein, E.A.S., Krischok, S., Janek, J., Endres, F., 2010. Plasma electrochemistry in ionic liquids: deposition of copper nanoparticles. Phys. Chem. Chem. Phys. 12 (8), 1750–1755.
Cruz, B.H., DíAz-Cruz, J.M., DíAz-Cruz, M.S., Ariño, C., Esteban, M., Tauler, R., 2001. Differential pulse polarographic study of the Pb(II) complexation by glutathione. J. Electroanal. Chem. 516 (1–2), 110–118.
Detsri, E., Seeharaj, P., 2017. Colorimetric detection of glutathione based on phthalic acid assisted synthesis of silver nanoparticles. Colloids Surf. 533, 125–132.
Ghani, S., Sharif, R., Bashir, S., Zaidi, A.A., Rafique, M.S., Ashraf, A., Shahzadi, S., Rafique, S., Kamboh, A.H., 2015. Polypyrrole thin films decorated with copper nanostructures as counter electrode for dye-sensitized solar cells. J. Power Sources 282, 416–420.
Gu, J., Hu, D., Wang, W., Zhang, Q., Meng, Z., Jia, X., Xi, K., 2015. Carbon dot cluster as an efficient "off-on" fluorescent probe to detect Au(III) and glutathione. Biosens. Bioelectron. 68, 27–33.
Gutscher, M., Pauleau, A.L., Marty, L., Brach, T., Wabnitz, G.H., Samstag, Y., Meyer, A.J., Dick, T.P., 2008. Real-time imaging of the intracellular glutathione redox potential. Nat. Methods 5 (6), 553–559.
Hakuna, L., Doughan, B., Escobedo, J.O., Strongin, R.M., 2015. A simple assay for glutathione in whole blood. Analyst 140 (10), 3339–3342.
Hu, B., Cao, X., Zhang, P., 2013. Selective colorimetric detection of glutathione based on quasi-stable gold nanoparticles assembly. New J. Chem. 37 (12), 3853–3856.
Ju, J., Zhang, R., He, S., Chen, W., 2014. Nitrogen-doped graphene quantum dots-based fluorescent probe for the sensitive turn-on detection of glutathione and its cellular imaging. RSC Adv. 4 (94), 52583–52589.
Kanďár, R., Vrbová, M., Čandová, J., 2013. An assay of total glutathione and glutathione disulfide in human whole blood and plasma using a high-performance liquid

chromatography with fluorescence detection. J. Liq. Chromatogr. Relat. Technol. 36 (14), 2013–2028.
Kong, F., Liang, Z., Luan, D., Liu, X., Xu, K., Tang, B., 2016. A glutathione (GSH)-responsive near-infrared (NIR) theranostic prodrug for cancer therapy and imaging. Anal. Chem. 88 (12), 6450–6456.
Li, R., Li, S., Dong, M., Zhang, L., Qiao, Y., Jiang, Y., Qi, W., Wang, H., 2015. A highly specific and sensitive electroanalytical strategy for microRNAs based on amplified silver deposition by the synergic TiO_2 photocatalysis and guanine photoreduction using charge-neutral probes. Chem. Commun. 51 (89), 16131–16134.
Liu, M., Zhang, L., Hua, Y., Feng, L., Jiang, Y., Ding, X., Qi, W., Wang, H., 2017. Mesoporous silver-melamine nanowires formed by controlled supermolecular self-assembly: a selective solid-state electroanalysis for probing multiple sulfides in hyperhaline media through the specific sulfide-chloride replacement reactions. Anal. Chem. 89 (17), 9552–9558.
Lv, Y., Yang, L.L., Mao, X.X., Lu, M.J., Zhao, J., Yin, Y.M., 2016. Electrochemical detection of glutathione based on Hg^{2+}-mediatedstrand displacement reaction strategy. Biosens. Bioelectron. 85, 664–668.
Miao, P., Liu, L., Nie, Y., Li, G., 2009. An electrochemical sensing strategy for ultrasensitive detection of glutathione by using two gold electrodes and two complementary oligonucleotides. Biosens. Bioelectron. 24 (11), 3347–3351.
Niu, L.Y., Guan, Y.S., Chen, Y.Z., Wu, L.Z., Tung, C.H., Yang, Q.Z., 2012. BODIPY-based ratiometric fluorescent sensor for highly selective detection of glutathione over cysteine and homocysteine. J. Am. Chem. Soc. 134 (46), 18928–18931.
Safavi, A., Maleki, N., Farjami, E., Mahyari, F.A., 2009. Simultaneous electrochemical determination of glutathione and glutathione disulfide at a nanoscale copper hydroxide composite carbon ionic liquid electrode. Anal. Chem. 81 (18), 7538–7543.
Shahmiri, M.R., Bahari, A., Karimi-Maleh, H., Hosseinzadeh, R., Mirnia, N., 2013. Ethynylferrocene–NiO/MWCNT nanocomposite modified carbon paste electrode as a novel voltammetric sensor for simultaneous determination of glutathione and acetaminophen. Sens. Actuators, B 177, 70–77.
Shi, F., Zheng, W., Wang, W., Hou, F., Lei, B., Sun, Z., Sun, W., 2015. Application of graphene–copper sulfide nanocomposite modified electrode for electrochemistry and electrocatalysis of hemoglobin. Biosens. Bioelectron. 64, 131–137.
Si, Y., Sun, Z., Zhang, N., Qi, W., Li, S., Chen, L., Wang, H., 2014. Ultrasensitive electroanalysis of low-level free MicroRNAs in blood by maximum signal amplification of catalytic silver deposition using alkaline phosphatase-incorporated gold nanoclusters. Anal. Chem. 86 (20), 10406–10414.
Sousa, A.A., Morgan, J.T., Brown, P.H., Adams, A., Jayasekara, M.P., Zhang, G., Ackerson, C.J., Kruhlak, M.J., Leapman, R.D., 2012. Synthesis, characterization, and direct intracellular imaging of ultrasmall and uniform glutathione-coated gold nanoparticles. Small 8 (14), 2277–2286.
Squellerio, I., Caruso, D., Porro, B., Veglia, F., Tremoli, E., Cavalca, V., 2012. Direct glutathione quantification in human blood by LC-MS/MS: comparison with HPLC with electrochemical detection. J. Pharm. Biomed. Anal. 71, 111–118.
Sun, Z., Li, S., Jiang, Y., Qiao, Y., Zhang, L., Xu, L., Liu, J., Qi, W., Wang, H., 2016. Silver nanoclusters with specific ion recognition modulated by ligand passivation toward fluorimetric and colorimetric copper analysis and biological imaging. Sci. Rep. 6, 20553.
Tan, M.X., Sum, Y.N., Ying, J.Y., Zhang, Y., 2013. A mesoporous poly-melamine-formaldehyde polymer as a solid sorbent for toxic metal removal. Energy Environ. Sci. 6 (11), 3254–3259.
Tsardaka, E.C., Zacharis, C.K., Tzanavaras, P.D., Zotou, A., 2013. Determination of glutathione in baker's yeast by capillary electrophoresis using methyl propiolate as derivatizing reagent. J. Chromatogr. A 1300, 204–208.
Tsoufis, T., Colomer, J.F., Maccallini, E., Jankovic, L., Rudolf, P., Gournis, D., 2012. Controlled synthesis of carbon-encapsulated copper nanostructures by using smectite clays as nanotemplates. Chem. Eur. J. 18 (30), 9305–9311.
Xu, H., Hepel, M., 2011. Molecular beacon-based fluorescent assay for selective detection of glutathione and cysteine. Anal. Chem. 83 (3), 813–819.
Yin, J., Kwon, Y., Kim, D., Lee, D., Kim, G., Hu, Y., Ryu, J.H., Yoon, J., 2014. Cyanine-based fluorescent probe for highly selective detection of glutathione in cell cultures and live mouse tissues. J. Am. Chem. Soc. 136 (14), 5351–5358.
Yin, M., Wu, C.K., Lou, Y., Burda, C., Koberstein, J.T., Zhu, Y., O'Brien, S., 2010. Copper oxide nanocrystals. J. Am. Chem. Soc. 36 (41), 9506–9511.
Yuan, Y., Zhang, J., Wang, M., Mei, B., Guan, Y., Liang, G., 2013. Detection of glutathione in vitro and in cells by the controlled self-assembly of nanorings. Anal. Chem. 85 (3), 1280–1284.
Zhang, H., Wang, C., Wang, K., Xuan, X., Lv, Q., Jiang, K., 2016. Ultrasensitive fluorescent ratio imaging probe for the detection of glutathione ultratrace change in mitochondria of cancer cells. Biosens. Bioelectron. 85, 96–102.
Zhao, Y., Xu, L., Li, S., Chen, Q., Yang, D., Chen, L., Wang, H., 2015. One-drop-of-blood electroanalysis of lead levels in blood using a foam-like mesoporous polymer of melamine–formaldehyde and disposable screen-printed electrodes. Analyst 140 (6), 1832–1836.
Zhu, S., Zhao, X.-e., Zhang, W., Liu, Z., Qi, W., Anjum, S., Xu, G., 2013. Fluorescence detection of glutathione reductase activity based on deoxyribonucleic acid-templated silver nanoclusters. Anal. Chim. Acta 786, 111–115.